Nonlinear structure-composition relationships in the $Ge_{1-y}Sn_y/Si(100)$ ($y < 0.15$) system

R. Beeler,[1] R. Roucka,[1] A. V. G. Chizmeshya,[1] J. Kouvetakis,[1] and J. Menéndez[2,*]
[1]*Department of Chemistry and Biochemistry, Arizona State University, Tempe, Arizona 85287-1604, USA*
[2]*Department of Physics, Arizona State University, Tempe, Arizona 85287-1504, USA*
(Received 21 February 2011; revised manuscript received 28 May 2011; published 26 July 2011)

The compositional dependence of the cubic lattice parameter in $Ge_{1-y}Sn_y$ alloys has been revisited. Large 1000-atom supercell *ab initio* simulations confirm earlier theoretical predictions that indicate a positive quadratic deviation from Vegard's law, albeit with a somewhat smaller bowing coefficient, $\theta = 0.047$ Å, than found from 64-atom cell simulations ($\theta = 0.063$ Å). On the other hand, measurements from an extensive set of alloy samples with compositions $y < 0.15$ reveal a negative deviation from Vegard's law. The discrepancy with earlier experimental data, which supported the theoretical results, is traced back to an unexpected compositional dependence of the residual strain after growth on Si substrates. The experimental bowing parameter for the relaxed lattice constant of the alloys is found to be $\theta = -0.066$ Å. Possible reasons for the disagreement between theory and experiment are discussed in detail.

DOI: 10.1103/PhysRevB.84.035204 PACS number(s): 61.66.Dk, 61.50.Ah, 81.05.Cy

I. INTRODUCTION

Linear interpolation between the parent compounds is the simplest approach for estimating the properties of semiconductor alloys. Although this scheme, in principle naïve, works surprisingly well for a variety of properties and material systems, applications that require very accurate values of certain parameters have prompted systematic studies of departures from linearity. A good example is the compositional dependence of band gaps. In laser or detector devices, the exact emission or cutoff wavelengths are of primary importance; therefore, even small deviations from linearity may be of practical significance in this context. Similarly, detailed knowledge of the deviations from Vegard's law[1] in the compositional dependence of the lattice constant can be used for accurate determinations of the alloy composition using x-ray diffraction (XRD).

The deviations from linear behavior in the compositional dependence of alloy properties are often characterized by introducing bowing parameters (quadratic coefficients). The magnitude of these bowing parameters has been successfully correlated with the mismatch in size and electronic properties between the constituent atoms.[2] For example, a comparative study of the optical properties of $Si_{1-x}Ge_x$ and $Ge_{1-y}Sn_y$ alloys[3] reveals much larger bowing parameters in the latter, which has been attributed to the larger difference in atomic sizes, as well as electronegativities. In the case of the cubic lattice parameter, a small negative deviation from linearity was observed in $Si_{1-x}Ge_x$ alloys,[4] whereas a small positive departure was reported for $Ge_{1-y}Sn_y$ alloys.[5] This qualitatively different behavior has been confirmed in a number of *ab initio* theoretical studies.[5–9]

The different signs of the bowing parameters in $Si_{1-x}Ge_x$ and $Ge_{1-y}Sn_y$ alloys provide a unique insight into the origin of the deviations from Vegard's law. Using a simple structural model of the alloys that assumes force constants independent of the bond nature, Mousseau and Thorpe showed that in a $Si_{1-x}Ge_x$ alloy the observed negative deviation from Vegard's law is obtained if the equilibrium heteronuclear Si-Ge bond length is smaller than the average of the homonuclear Si-Si and Ge-Ge lengths.[10] However, they were unable to confirm that this is the main cause of bowing, because they lacked an independent way to determine the equilibrium bond lengths and they could not rule out other factors, such as different force constants or clustering effects. Strong evidence for the bond length origin of the bowing was provided by Chizmeshya *et al.*, who studied solid-state systems and molecular analogs consisting of tetrahedral clusters of the form $A(BH_3)_4$, where A and B can be C, Si, Ge, or Sn.[5] Their crucial finding is that the difference between heteronuclear and average homonuclear bonds in the molecular compounds is about the same, in magnitude and sign, as in the corresponding solid phases. In particular, the trends in the molecular compounds are in perfect agreement with the predicted positive bowing in $Ge_{1-y}Sn_y$ alloys and negative bowing in $Si_{1-x}Ge_x$ alloys.

Although the work of Chizmeshya *et al.* provides a convincing framework for understanding the origin of bowing in the compositional dependence of the lattice constant in group IV alloys,[5] the problem cannot be considered definitively solved because the smallness of the quadratic terms make their theoretical evaluation and experimental determination quite challenging. On the theoretical side, earlier *ab initio* theoretical calculations for $Si_{1-x}Ge_x$ alloys indicated a positive deviation from linearity,[11] in disagreement with the experimental results from Dismukes *et al.*[4] and with more recent calculations.[12,13] This suggests that convergence issues, as well as artificial correlations introduced by the small supercells used to simulate the alloy, may affect the predicted deviations from linearity. Accordingly, we have carried out *ab initio* lattice constant calculations in very large (1000 atom) supercells, which provide a statistically accurate description of the random alloy. We optimized the supercell cell shape, dimensions, and internal atomic positions to obtain highly converged equilibrium structures, with residual cell stresses <1 kbar and atomic forces <0.005 eV/Å. These calculations confirm the earlier predictions of a positive deviation from Vegard's law.

On the experimental side, the problem is particularly difficult because bulklike $Ge_{1-y}Sn_y$ samples are not available and the measurements must be performed on epitaxial alloys on Si substrates. A good illustration of the experimental difficulties associated with thin film measurements is provided by the

work of Kasper *et al.,*[14] who determined the lattice parameter in $Si_{1-x}Ge_x$ films grown pseudomorphically on Si and could only verify Dismukes's earlier bulk data[4] in a semiquantitative way because of the uncertainties in the Ge concentrations and in the strain corrections. In the case of $Ge_{1-y}Sn_y$ alloys, the experimental evidence so far is based on measurements of $Ge_{1-y}Sn_y$ films grown directly on (001) Si.[5] In this work, the c lattice constant perpendicular to the growth plane was obtained from the (004) x-ray reflection in the tetragonally distorted diamond structure. In view of the low residual strain in the samples, the measured c was identified with the relaxed cubic lattice constant a_0. The systematic error incurred by using this approximation does not affect the sign of the quadratic term in the compositional dependence of the lattice constant as long as the residual strain can be assumed to be the same for all samples, a reasonable assumption at the time. In subsequent years, however, we have accumulated increasing evidence that this residual strain is strongly correlated with the alloy composition, to the extent that a systematic error might be introduced in the determination of the bowing parameters for the alloy if a strain correction is not applied. In view of these complications, we have measured x-ray reciprocal space maps (RSMs) of the (224) reflection for a large set of $Ge_{1-y}Sn_y$ alloys grown on Si substrates. We extract the relaxed cubic lattice parameter from these measurements, and we find that the deviation from Vegard's law is negative. Thus, we conclude that that there is a remaining disagreement between theory and experiment in the case of $Ge_{1-y}Sn_y$ alloys. The experimental lattice constant bowing parameter for the $Ge_{1-y}Sn_y$ alloy, however, is less than the bowing parameter for the $Si_{1-x}Ge_x$ alloy as a fraction of the lattice constant mismatch between the parent elemental semiconductors, whereas the bowing parameters for all other measured properties are much larger in $Ge_{1-y}Sn_y$ than in $Si_{1-x}Ge_x$. This suggests that the data may be viewed as qualitative confirmation of theory if we assume that the predicted trend to positive bowing in $Ge_{1-y}Sn_y$ alloy is overcompensated by an intrinsic or extrinsic contribution that is unaccounted for in the theoretical simulations.

The remainder of the paper is organized as follows: in Sec. II we present the new theoretical simulations, in Sec. III we present the new experimental data, and in Sec. IV we discuss the divergent conclusions from theory and experiments and analyze possible reasons for the discrepancy.

II. THEORY

For the alloy simulation, we adopted 1000-atom supercells composed of a $5 \times 5 \times 5$ array of conventional 8-atom crystallographic cells, in which the Sn and Ge atoms are randomly distributed on the available sites. We specifically consider two alloy compositions: the first containing 50% Sn, where any deviations from average behavior are expected to be close to maximal, and a 10% Sn model, which overlaps with the high end of the composition range explored in our study. The latter is expected to provide a useful point of comparison with experiment. The 1000-atom supercell models represent a significant refinement over our earliest calculations for this system in which much smaller 64-atom supercells were used to describe Sn_yGe_{1-y} alloy compositions with Sn content from 0%–50%.[5] In this case, however, highly symmetric ordered atomic distributions were used to make the calculations tractable. In subsequent work on related $Si_{1-y}Sn_y$ alloys, we incorporated the random nature of the alloys using both discrete 64-atom distributions and special quasirandom cells.[15] In this regard, the present treatment using the very large supercells is expected to inherently capture most random lattice pair correlations up to about the sixth nearest neighbor. As we show later, our $Ge_{1-y}Sn_y$ simulations yield nearly Gaussian bond species distributions, which follow the expected limiting statistical behavior based on concentration products, i.e., y^2, $2y(1-y)$, and $(1-y)^2$ for Sn-Sn, Sn-Ge, and Ge-Ge bonds, respectively. For a 1000-atom diamond lattice unit cell, the number of bonds is 2000 (e.g., 4 bonds per tetrahedral site times $\frac{1}{2}$ for double counting). For 10% Sn concentration, our $Ge_{1-y}Sn_y$ alloy representation should contain 20 Sn-Sn bonds, 360 Sn-Ge bonds, and 1620 Ge-Ge bonds. In practice, we find that our random configurations contain distributions that deviate from these ideal values by only 1 or 2 bonds, suggesting that our approach should be sufficient to capture the essential structural properties of real alloys.

The ground state energy calculations of the random alloys and elemental Ge and Sn lattices were all carried out using the Vienna *ab initio* simulation package (VASP) electronic structure code.[16,17] We employed the Ceperley-Alder (CA) parameterization of the local density approximation (LDA) functional[18,19] for exchange-correlation energy, a plane wave cutoff of 350 eV, and a single k point centered at Γ, which is found to be adequate in view of the large lattice dimensions ($\sim$30 Å). Special precautions were taken to ensure that the calculations of the elemental α-Ge and α-Sn reference system properties and those of the alloys are performed consistently and at the same level of fidelity. In particular, we ensured that all internal integration grids and sampling procedures were identical in all cases. Using these computational conditions, we then simultaneously optimized the supercell shape and dimensions, as well as the atomic positions, to obtain very accurate equilibrium structures with residual cell stress and atomic forces of less than $\sim$1 kbar and $\sim$0.005 eV/Å, respectively.

The key outcomes of our study are summarized in Table I, which lists the electronic ground state energies U_0 and lattice parameters a_0 for the elemental reference states (α-Ge and α-Sn), as well as the compositionally average (Vegard) values corresponding to 10% and 50% Sn content. Energies produced by VASP (listed here as U_0) are relative to spin-compensated neutral atoms, not spin-polarized ground state configurations. All lattice constants listed in the table correspond to a conventional crystallographic cell and were obtained by dividing the supercell edge length by 5 (small distortions in edge length of $\sim$0.001 Å were averaged). Our LDA values for the lattice constants of α-Ge and α-Sn are, respectively, 0.57% and 0.49% smaller than their corresponding experimental values at room temperature. Because the calculations correspond to static values, a more meaningful comparison is with low-temperature lattice constants corrected for zero-point vibrational expansion. The experimental static values are extrapolated from the asymptotically linear temperature dependence observed

TABLE I. Summary of energetic and structural results for the $Ge_{1-y}Sn_y$ supercell calculations.

	U_0 (eV/atom)	ΔU (eV/atom)	ΔG (eV/atom)[a]	a_0 (Å)	Δa_0 (Å)
α-Sn	−4.5008	—	—	6.4574	—
	−4.5016[b]			6.4557[b]	
				6.4894[c]	
α-Ge	−5.1969	—	—	5.6250	—
	−5.1980[b]			5.6261[b]	
				5.6574[c]	
ySn + $(1-y)$Ge ($y = 0.5$)	−4.8489	—	—	6.0412	—
ySn + $(1-y)$Ge ($y = 0.1$)	−5.1273	—	—	5.7082	—
α-$Ge_{0.9}Sn_{0.1}$ (RAND)	−5.1079	+0.0194	+0.0110	5.7127	0.0045
α-$Ge_{0.5}Sn_{0.5}$ (RAND)	−4.8009	+0.0480	+0.0301	6.0529	0.0117
α-$Ge_{0.5}Sn_{0.5}$ (ZB)	−4.8197	+0.0292	+0.0292	6.0522	0.0110

NOTE : RAND = random; ZB = zincblende.

[a]The free-energy estimates ΔG are obtained by combining the molar mixing enthalpy and an ideal mixing formula for mixing entropy at $T =$ 300K.

[b]Values from our prior study (Ref. 5) using 64-atom cell representations for α-Ge and α-Sn.

[c]Experimental values at room temperature, shown in italics.

at high temperatures;[20] proceeding this way, we find that the differences between theory and experiment are reduced to 0.46% (α-Ge) and 0.35% (α-Sn). The residual discrepancy is typical for this level of density-functional theory (DFT). Also listed in the table are values from our prior work, which were obtained using a similar DFT treatment at the CA-LDA level using the much smaller 64-atom setting but higher cutoff energy (600 eV) and $3 \times 3 \times 3$ Monkhorst-Pack sampling for reciprocal space integrations. The agreement is clearly good, and the small discrepancies result entirely from the different computational conditions used.

The bottom portion of Table I summarizes the key energetic and structural results for the alloys, including their equilibrium lattice constants a_0 and ground state electronic energies U_0, as well as corresponding deviations from compositionally weighted average (Vegard) values (Δa_0 and ΔU, respectively). The arbitrary spin-compensated *atomic* reference states (discussed earlier), contained in the U_0 values generated by VASP, cancel out one another in the calculation of ΔU. Accordingly, the latter represent the electronic contribution to the formation energies of a $Ge_{1-y}Sn_y$ alloy relative to its pure Sn and Ge end members. On the basis of the calculated ΔU listed here, the 10% and 50% random SnGe alloys are predicted to be metastable by ∼19 and ∼48 meV/atom, respectively. Also listed for comparison is the corresponding ΔU value of ∼29 meV/atom for the symmetric zinc-blende configuration of the $Ge_{0.5}Sn_{0.5}$ alloy, which is found here to possess a slightly lower (i.e., less metastable) electronic energy than the corresponding random alloy. To more quantitatively describe the thermodynamic stability of the alloys, we calculated the alloy Gibbs free energy $G = H - TS$. For simplicity, we ignore the vibrational contributions to the free energy (assumed to be small in comparison to ΔU) and approximate the alloy enthalpy of mixing as $\Delta H^{\mathrm{MIX}}_{\mathrm{SnGe}}(y) = U_0^{\mathrm{SnGe}}(y) - yU_0^{\mathrm{Sn}} - (1-y)U_0^{\mathrm{Ge}}$. For the corresponding entropy contribution to the free energy, we assume an ideal mixing formula, $TS^{\mathrm{MIX}}_{\mathrm{GeSn}}(y) = -k_B T[y \ln y + (1-y)\ln(1-y)]$, which yields 8.40 and 17.92 meV/atom for the 10% and 50% random alloys, respectively. With these approximations, the Gibbs free energy ΔG levels of the random and ordered systems are predicted to be nearly identical, differing by only a few millielectron volts per atom near ambient conditions, while at higher temperatures the mixing entropy is expected to favor the random alloy.

The equilibrium lattice constants a_0 of the alloys obtained from our simulation are listed in the bottom right-hand portion of the table, along with their corresponding deviations from compositionally averaged (Vegard) values, Δa_0. For both compositions, the deviations are predicted to be positive, and the nominal bowing parameter, assuming a dependence of the form

$$a_0(y) = a_0^{\mathrm{Ge}}(1-y) + a_0^{\mathrm{Sn}} y + \theta^{\mathrm{GeSn}} y(1-y), \qquad (1)$$

is found to be $\theta^{\mathrm{GeSn}} = 0.0468$ Å, quite close to the value $\theta^{\mathrm{GeSn}} = 0.063$ Å reported in our earlier study on $Ge_{1-y}Sn_y$,[5] as well as in other studies.[6,8] The bowing parameter obtained in the present study for the perfectly ordered zinc-blende configuration is $\theta^{\mathrm{GeSn}} = 0.0440$ Å, which is perhaps surprising in view of its radically different bonding topology (e.g., the presence of exclusively Sn-Ge bonds).

Equilibrium structures for the calculated alloys are shown in Fig. 1, where the Sn atoms are represented by gray spheres and the tetrahedral lattice, including the Ge atoms, is drawn using faint (blue) lines. The supercell parameters a_{SC} and lattice constants $a = a_{\mathrm{SC}}/5$ are listed below these figures. The parameter $\langle b \rangle_{\mathrm{SC}}$ provided above the structure model represents an "intrinsic bond length" obtained from the macroscopic cell dimension ($\frac{\sqrt{3}}{4}a$). In the zinc-blende structure (and elemental diamond lattices), $\langle b \rangle_{\mathrm{SC}}$ is precisely equal to the unique tetrahedral bond length in the system. The Ge-Ge, Sn-Ge, and Sn-Sn bond distributions obtained from our 1000-atom simulations of the 10% and 50% Sn alloys are plotted in the right panels of Fig. 1, which exhibit nearly Gaussian forms for all species. The mean bond length

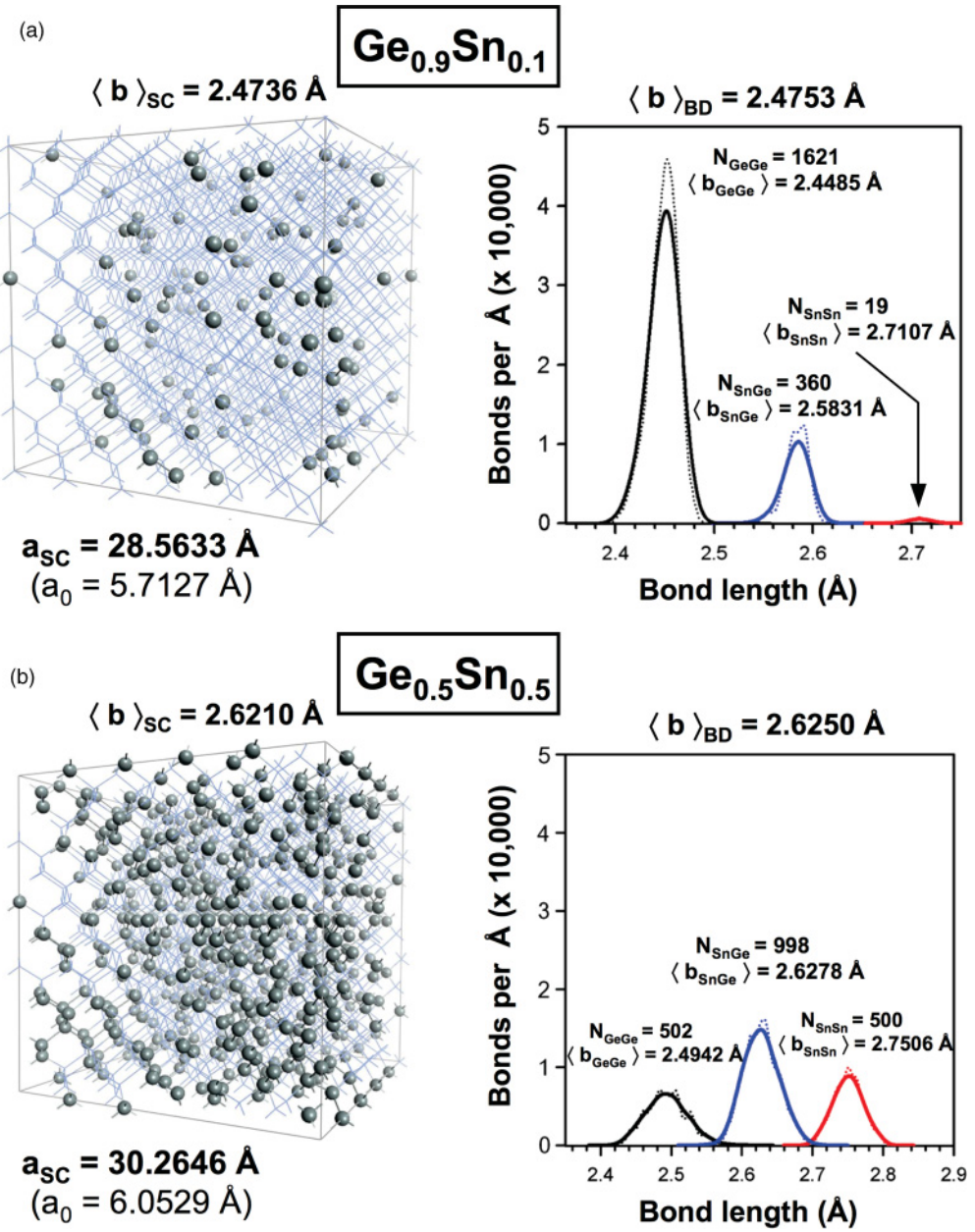

FIG. 1. (Color online) Bond distribution analysis of the $Sn_{0.1}Ge_{0.9}$ (a) and $Sn_{0.5}Ge_{0.5}$ (b) random alloy models. Representative structures for the alloys are shown in the left panels, with the diamond lattice, including Ge positions, drawn using faint (blue) lines and gray spheres representing the Sn atoms. Plots on the right show the corresponding distributions for GeGe (black), SnGe (blue), and SnSn (red) bonds. The number of bonds and mean bond lengths for each species are indicated within the figures. The values $\langle b \rangle_{BD}$ and $\langle b \rangle_{SC}$ are the average bond lengths obtained from the weighted bond distributions and the macroscopic crystal dimensions, respectively.

$\langle b \rangle_{ij}$ listed above each distribution function is calculated by dividing the first moment of the distribution by its integrated area (equal to the number of bonds, listed as N_{ij}). Finally, above each plot we list the mean bond length $\langle b \rangle_{BD}$ obtained for each alloy from the weighted sum of individual mean bond lengths $\langle b \rangle_{ij}$. For disordered binary alloy systems such as $Ge_{1-y}Sn_y$, characterized by relatively compressible bonds, our simulations correctly embody the fundamental deviations of bonds lengths from their natural values as deduced from the elemental end members and interpolation between these latter values. Variations on the order of 2%–4% are typical, as illustrated in Table II, which lists the characteristic Ge-Ge, Sn-Ge, and Sn-Sn bond lengths obtained from our simulations of elemental Ge and Sn and the GeSn alloys.

III. EXPERIMENT

$Ge_{1-y}Sn_y$ films were grown on (001) Si substrates via reactions of SnD_4 with Ge_2H_6, as described elsewhere.[21] Rutherford backscattering (RBS) via the Rutherford Universal Manipulation Program (RUMP) was used to determine the Sn concentration and film thickness,[22] which varied from ~800 nm for the lowest Sn concentrations to ~90 nm for $y = 0.13$. The calculated areal density is obtained by modeling

TABLE II. Characteristic bond lengths (in Å) in the $Ge_{1-y}Sn_y$ alloys and elemental Sn and Ge calculated using 1000-atom supercells.

	Ge-Ge	Sn-Ge	Sn-Sn
α-Ge	2.436	—	—
$Ge_{0.9}Sn_{0.1}$	2.449	2.583	2.711
$Ge_{0.5}Sn_{0.5}$	2.494	2.628	2.751
α-Sn	—	—	2.796

the system as a diamond-structure $Ge_{1-y}Sn_y$ alloy. This approach is found to perfectly reproduce the thickness of the layers as measured by cross-sectional transmission electron microscopy (XTEM) and from ellipsometric determinations. In typical acquisition of the random spectrum, the sample is continuously rotated to avoid channeling. Typically, 10^5 counts are collected at a beam energy of 0–2 MeV corresponding to 350 channels, which ensure a high signal-to-noise ratio sufficient for resolving Sn contents as low as 0.1%. This technique is ideally suited for these binary alloys, because the atomic number of each constituent element is high and sufficiently distinct to enable a clear (unambiguous) separation of their signals.

In addition to thickness and composition, the degree of crystallinity and epitaxial alignment of the films is gauged by RBS analysis using the ratio of the aligned versus random peak heights (χ_{min}). In our samples, it decreases from 10% at the interface to 5% at the surface, indicating a reduction in dislocation density across the thickness of the film. The 5% value approaches the limit of $\chi_{min} \approx 3\%$ observed in a perfect Si crystal, suggesting that most defects accommodating the lattice mismatch between film and substrate are confined at the interface. This is consistent with XTEM micrographs showing essentially defect-free films. The concentration of residual threading defects and the mosaic spread of the crystal are improved by performing a few—typically three—rapid-thermal annealing (RTA) cycles of 2–30 s each at temperatures between 600 °C and 750 °C. This postgrowth processing reduces the full width at half maximum of the (004) rocking curve in high-resolution x-ray diffraction (HR-XRD) measurements.

The HR-XRD measurements of the lattice constant were carried out at room temperature using a PANalytical diffractometer. The in-plane a and perpendicular c tetragonal lattice parameters of 56 $Ge_{1-y}Sn_y$ samples and 14 reference Ge films on Si were determined from measurements of the (004) $2\theta/\omega$ peaks and RSMs of the (224) reflection. The pure Ge films had a range of thicknesses comparable to those of the $Ge_{1-y}Sn_y$ alloys and were grown using the method described in Ref. 23. The samples were first aligned to the Si (004) reflection, and the position of the $Ge_{1-y}Sn_y$ (004) peak was measured. From the $Ge_{1-y}Sn_y$ (004) peak position, the c lattice parameter and a possible lattice tilt were calculated. In all cases, the tilt was found to be negligible. After that, the sample was aligned to the corresponding Si (224) reflection and the $Ge_{1-y}Sn_y$ (224) reflection was measured. The in-plane and out-of-plane lattice parameters were determined from the 224 peak maxima. For a subset of the samples we measured the four (224), $(\bar{2}24)$,$(2\bar{2}4)$, and $(\bar{2}\bar{2}4)$ reflections to confirm the tetragonal nature of the distortion and establish a limit for the inherent error of the method. All c lattice parameters determined from (224) reflections were found to match the value obtained from the (004) reflections to within 0.0004 Å. The relaxed cubic lattice constant a_0 was computed from the measured a and c parameters using

$$a_0 = \frac{c + \frac{2C_{12}}{C_{11}}a}{1 + \frac{2C_{12}}{C_{11}}}, \tag{2}$$

where C_{11} and C_{22} are cubic elastic constants in the contracted index notation. The elastic constant ratio is taken as

$$\frac{C_{12}}{C_{11}} = 0.3738 + 0.1676y - 0.0296y^2. \tag{3}$$

The independent term in Eq. (3) is the value of C_{12}/C_{11} in pure Ge, as reported by McSkimin.[24] The compositional dependence of C_{12}/C_{11} was obtained from a quadratic interpolation of the *ab initio* theoretical calculations in Ref. 25.

For the pure Ge films on Si, the use of Eqs. (2) and (3) gives $a_0 = 5.6571 \pm 0.0004$ Å. This is in good agreement with the value $a_0 = 5.6574$ Å quoted in Ref. 26 as the average of all data for pure Ge compiled from 1922 to 1968. For the samples for which the four (224) were measured, the relaxed lattice parameters a_0 were found to be nearly identical, with typical standard deviations of ~0.0001 Å. In Fig. 2 we show the a, c, and a_0 values for the $Ge_{1-y}Sn_y$ samples. The calculated value of a_0 for the alloys is in principle affected by the accuracy of the compositional dependence of the elastic constant ratio in Eq. (3), for which there is no experimental corroboration. However, the exact value of C_{12}/C_{11} is not as critical as in the $Si_{1-x}Ge_x$ experiments reported in Ref. 14, because the strain levels in our samples are about one order of magnitude lower; therefore, the uncertainties in the compositional dependence

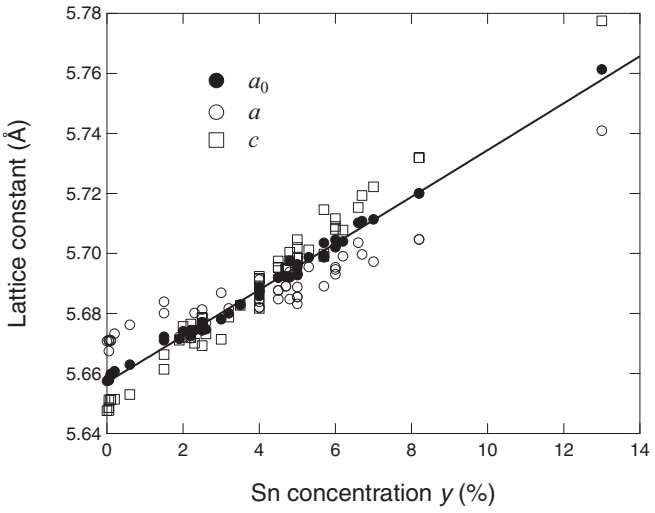

FIG. 2. Experimental lattice constants a (parallel to growth plane) and c (perpendicular to the growth plane) obtained from room-temperature HR-XRD RSM measurements of $Ge_{1-y}Sn_y$ films on Si. The relaxed cubic lattice constant a_0 is calculated from these values using Eqs. (2) and (3). The solid line is a fit with Eq. (1). The residual strain is tensile ($a > c$) for low Sn concentrations and becomes compressive ($a < c$) for high Sn concentrations.

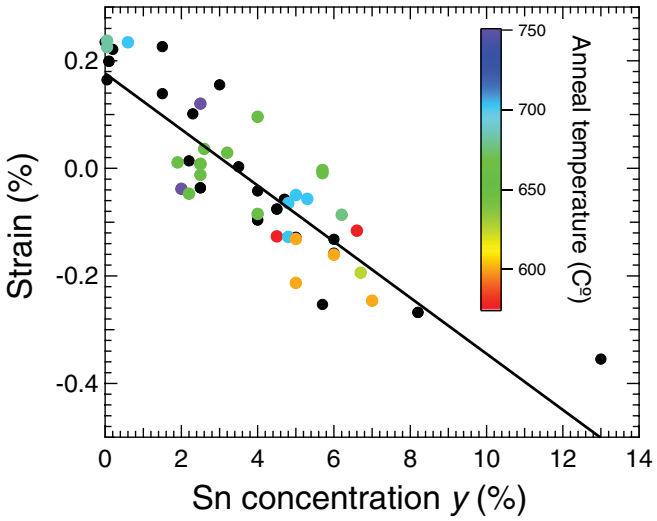

FIG. 3. (Color) In-plain strain $\varepsilon_{\parallel} = (a - a_0)/a_0$ computed from the data in Fig. 2 for all $Ge_{1-y}Sn_y$ samples. The color code indicates the after-growth RTA temperatures for the different samples. Black circles correspond to samples measured as grown without RTA treatment. The line is a linear fit to the strain.

of the elastic constant ratio have a substantially reduced impact on the final a_0 value. The bowing parameter for the compositional dependence of a_0 (discussed later) remains virtually unchanged if we ignore the composition-dependent terms in Eq. (3) and simply use the pure Ge value from McSkimin.[24]

It is apparent from Fig. 2 that for low Sn concentrations $a > c$, whereas for high Sn concentrations $a < c$. This indicates a gradual transformation of the nature of the in-plane strain $\varepsilon_{\parallel} = (a - a_0)/a_0$ from tensile at low Sn concentrations to compressive at the highest Sn concentrations, as shown in Fig. 3.

If the films are perfectly relaxed during growth, we would expect the residual strain at room temperature to be tensile because of the smaller thermal expansion coefficient of the Si substrate relative to the $Ge_{1-y}Sn_y$ film. This is in fact the approach used to obtain tensile-strained Ge films on Si.[27] The presence of compressive strain indicates an incomplete strain relaxation while the sample is growing. Although the higher Sn concentration may by itself inhibit the generation of the required misfit dislocations, the most likely reason for the incomplete strain relaxation is the lower growth temperatures used to deposit films with high Sn concentrations. These lower temperatures also reduce the growth rate, which leads to a monotonic decrease in film thickness as a function of the Sn concentration. Thus, we cannot rule out the possibility that the degree of strain relaxation during growth depends not only on the growth temperature but also on film thickness. Interestingly, our postgrowth annealings increase the tensile strain only marginally, as seen in Fig. 3, even though the annealing temperatures are much higher than the film growth temperatures. At even higher annealing temperatures, we expect the samples to relax and develop tensile strain upon cooling to room temperature, regardless of the growth temperature. The threshold annealing temperature for this behavior seems to be close to 725 °C for pure Ge films, but this limit is difficult to explore in $Ge_{1-y}Sn_y$ alloys because the Sn concentration may change at the highest temperature annealings.

The simplest way to show that the data in Fig. 2 deviate from Vegard's law is to fit the a_0 values to a linear function of composition. This fitting gives $a_0(0) = 5.6571 \pm 0.0004$ Å, which is in perfect agreement with the directly measured Ge lattice constant, but $a_0(1) = 6.428 \pm 0.010$ Å for α-Sn, which is substantially *below* the experimental value $a_0 = 6.4894$ Å at 300K.[28] This clearly indicates a negative deviation from Vegard's law. The disagreement with the earlier finding of a positive deviation can be traced back to the measured c parameter increasing faster than a_0 as a function of Sn concentration, as seen in Fig. 2, because of the monotonic change in the residual strain from tensile to compressive. The solid line in Fig. 2 shows a fit with Eq. (1). Because the compositional range of the data is limited, a fit that uses a_0^{Ge}, a_0^{Sn}, and θ^{GeSn} as adjustable parameters gives a negative value for θ^{GeSn}, as expected, but an unphysical value for a_0^{Sn}. We thus perform the fit using $a_0^{Sn} = 6.4894$ Å as a fixed parameter; to treat both end values on equal footing, we also use a fixed $a_0^{Ge} = 5.6571$ Å. We are then left with θ^{GeSn} as the only adjustable parameter, and we obtain $\theta^{GeSn} = -0.066 \pm 0.005$ Å. We have verified that the value of θ^{GeSn} remains virtually unchanged if we use any of the published values for the lattice constant of α-Sn (similarly, if we use a_0^{Ge} as an adjustable parameter, we obtain $a_0^{Ge} = 5.6573 \pm 0.0004$ Å and $\theta^{GeSn} = -0.069 \pm 0.009$ Å). The deviation from Vegard's law $\Delta a_0 = a_0(y) - a_0^{Ge}(1 - y) - a_0^{Sn} y$ is shown in full detail in Fig. 4.

IV. DISCUSSION

The significance of the discrepancy between the theoretical predictions and the new measurements for $Ge_{1-y}Sn_y$ is difficult to assess. If we assume that the experimental compositional dependence of the deviation from Vegard's law is quadratic (hardly obvious from our data, given the noise

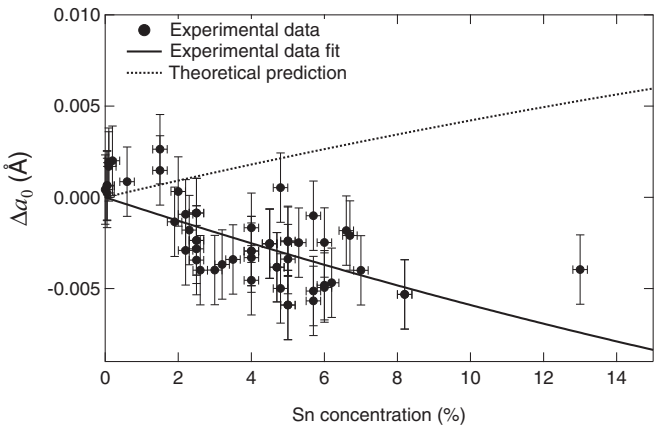

FIG. 4. Deviation Δa_0 from Vegard's law for the lattice constant of $Ge_{1-y}Sn_y$ alloys. The lines correspond to the function $\theta^{GeSn}\, y(1 - y)$. For the solid line, we use $\theta = -0.066$ Å from our a_0 fit in Fig. 2. The dotted line corresponds to the theoretical value $\theta^{GeSn} = +0.0468$ Å. The error bars assume an error of ±0.2% in the composition determined by RBS.

and the limited compositional range), the difference between the predicted and the actual lattice constant for $Ge_{0.5}Sn_{0.5}$ would be 0.46%, which is comparable to the error in the best DFT-LDA predictions of lattice constants. On the other hand, DFT-LDA calculations seem to correctly predict bowing in other semiconductor alloy systems, so the discrepancy in the case of $Ge_{1-y}Sn_y$ is puzzling. Moreover, the predicted lattice constant error for α-Sn is less than that for Ge. If we assume a correction factor that depends linearly on the alloy composition, this would add an additional small but *positive* contribution to the bowing, increasing the discrepancy with theory. The agreement is better at the lowest Sn concentrations ($y < 0.02$), as seen in Fig. 4. This could be fortuitous, given the limited number of data points and large error bars, but we have already found that at these same low Sn concentrations the bowing parameter for the direct electronic gap E_0 appears to be significantly larger than the value obtained from samples with $y > 0.02$.[29,30] These observations, taken together, suggest that some structural change might take place near $y \approx 0.02$. S-shaped deviations from Vegard's law have been explained in terms of the contribution from bond-bending forces.[31] For sufficiently large values of these forces, the bonds are prevented from expanding or compressing following atomic substitutions. However, because such effects are automatically included in *ab initio* calculations, we should have observed some anomaly in the theoretical compositional dependence of both lengths if the deviation from Vegard's law has an oscillating behavior as a function of the Sn concentration. A convenient way to study bond lengths in terms of the competition between bond-bending and bond-stretching forces is provided by the so-called topological rigidity parameter a^{**}.[32] This parameter measures of the difference between interatomic bond lengths and the macroscopic lattice constant—a relevant and useful figure of merit for the comparison of structural properties within a compositional family of alloys. A value of $a^{**} = 0$ corresponds to the completely rigid lattice (Vegard limit), in which bond-bending forces dominate and bonds lengths take on equal values to match the macroscopic lattice parameter. The opposite $a^{**} = 1$ case represents the so-called Pauling limit, in which bond-stretching forces are dominant, so that all bond length species take on their natural values and bond angle deviations accommodate the competition between macroscopic dimensions and local bond lengths. For a $Ge_{1-y}Sn_y$ alloy, a^{**} can be deduced by fitting the bond distributions for various compositions y in a random alloy to the formulas

$$\begin{aligned} \langle b_{\mathrm{GeGe}} \rangle &= \tilde{b} - y a^{**} \left(b^0_{\mathrm{SnSn}} - b^0_{\mathrm{GeGe}} \right), \\ \langle b_{\mathrm{SnSn}} \rangle &= \langle b_{\mathrm{GeGe}} \rangle + a^{**} \left(b^0_{\mathrm{SnSn}} - b^0_{\mathrm{GeGe}} \right), \\ \langle b_{\mathrm{SnGe}} \rangle &= \tfrac{1}{2} [\langle b_{\mathrm{GeGe}} \rangle + \langle b_{\mathrm{SnSn}} \rangle], \end{aligned} \tag{4}$$

where the b^0 are the natural (unique) bond lengths obtained from the pure phases, and the average bond length is defined as $\tilde{b} = y b^0_{\mathrm{SnSn}} + (1-y) b^0_{\mathrm{GeGe}}$. Using the data provided in Fig. 1 and Table II, our 1000-atom simulations yields $a^{**} = 0.685$ for $Ge_{0.9}Sn_{0.1}$ and $a^{**} = 0.693$ for $Ge_{0.5}Sn_{0.5}$. These values are remarkably consistent in view of the significant difference in Sn content between the two alloys and similar to the corresponding average value of $a^{**} \approx 0.68$ obtained in our prior studies on 12 GeSn alloy compositions between 0% and 50% Sn using 64-atom supercells.[5,15] Shen *et al.*[6] also reported a value of $a^{**} \approx 0.69$ for the $Ge_{1-y}Sn_y$ alloy on the basis of three compositions ($y = 0.25$, 0.50, and 0.75) using a 72-atom supercell setting. Collectively, the foregoing evidence suggests a universal value of $a^{**} = 0.69$ for $Ge_{1-y}Sn_y$ based on DFT-LDA. Thus, the ratio of bond-bending to bond-stretching forces seems to be independent of the composition, which is incompatible with an oscillating dependence of the deviation from Vegard's law near the low-Sn compositional range. Recently we also carried out a comparative topological rigidity analysis of the bonding in $Si_{1-y}Sn_y$ alloys[15] (also using 64-atom supercells) and obtained a value of $a^{**} \approx 0.72$. Direct experimental measurements of a^{**} are extremely difficult and only available for the $Si_{1-x}Ge_x$ alloy, where values of a^{**} in the range of 0.6–0.8 have been reported in the literature.[11,33–35]

Yet another interpretation of the discrepancy between theory and experiment would be to assume that the observed deviation from Vegard's law is caused by the combined effects of a positive contribution, as calculated for a perfectly random alloy, plus a negative term associated with a nonrandom atomic distribution and/or defects. This is suggested by the observation that the ratio $\eta^{\mathrm{GeSn}} = \theta^{\mathrm{GeSn}}/(a_0^{\mathrm{Sn}} - a_0^{\mathrm{Ge}})$, which measures the size of the nonlinear deviation relative to the lattice mismatch between the parent materials, is $\eta^{\mathrm{GeSn}} = 0.089$, whereas the equivalent quantity for $Si_{1-x}Ge_x$ alloys is $\eta^{\mathrm{SiGe}} = 0.12$. Because we find $\eta^{\mathrm{SiGe}} < \eta^{\mathrm{GeSn}}$ for the electronic properties,[3] the observation that $\eta^{\mathrm{SiGe}} > \eta^{\mathrm{GeSn}}$ for the lattice constant could be viewed as a qualitative confirmation of the theoretical predictions under a scenario in which the trend toward positive bowing is overcompensated for by the second effect.

A good measure of the importance of randomness in the predicted alloy lattice constants is provided by a comparison of a_0 calculated for the random $Ge_{0.5}Sn_{0.5}$ alloy and for the ordered zinc-blende GeSn compound. The finding that these lattice constants are nearly identical suggests that ordering effects do not play a dominant role in this system. On the other hand, the so-called Sn-split vacancies, in which Sn atoms are located at the bond-center site between two missing Ge atoms,[36] lead to a decrease in the lattice parameter. For example, Ventura *et al.* found a cubic lattice parameter of 5.77 Å for pure Ge, 5.82 Å for a $Ge_{15}Sn_1$ alloy, and 5.72 Å for a $Ge_{14}Sn_1$ alloy with a split vacancy.[37] The abundance of these defects is related to the vacancy concentration,[38] which may not be constant as a function of Sn concentration because of the different growth temperatures. Based on the Ventura *et al.* results,[37] we estimate that ~6% of the Sn atoms in the alloy should be in split vacancy locations to explain the difference between the observed and the predicted lattice parameter for $y = 0.06$. This is a much higher concentration of split vacancies than predicted by these authors, and it constitutes a level of nonsubstitutionality that likely would have been detected in our XRD or RBS channeling experiments.

V. CONCLUSIONS

We have revisited the compositional dependence of the lattice constant in $Ge_{1-y}Sn_y$ alloys from a theoretical and ex-

perimental perspective. Although the theoretical calculations confirm the positive deviation from Vegard's law predicted by earlier work, the experimental results indicate a clear negative deviation, in contradiction with earlier data that were affected by the residual strain in $Ge_{1-y}Sn_y$ films grown on Si. Different scenarios have been analyzed to explain the discrepancy, but no fully satisfactory explanation can be provided at this time.

ACKNOWLEDGMENTS

This work was supported by the US Air Force under Contract No. DOD AFOSR FA9550-06-01-0442 (Multidisciplinary University Research Initiative), by the US Department of Energy under Contract No. DE-FG36-08GO18003, and by the National Science Foundation under Grant No. DMR-0907600.

*jose.menendez@asu.edu

[1] L. Vegard, Zeits. Phys. **5**, 17 (1921).
[2] J. E. Bernard and A. Zunger, Phys. Rev. B **36**, 3199 (1987).
[3] V. R. D'Costa, C. S. Cook, A. G. Birdwell, C. L. Littler, M. Canonico, S. Zollner, J. Kouvetakis, and J. Menendez, Phys. Rev. B **73**, 125207 (2006).
[4] J. P. Dismukes, L. Ekstrom, and R. J. Paff, J. Phys. Chem. **68**, 3021 (1964).
[5] A. V. G. Chizmeshya, M. R. Bauer, and J. Kouvetakis, Chem. Mater. **15**, 2511 (2003).
[6] J. Shen, J. Zi, X. Xie, and P. Jiang, Phys. Rev. B **56**, 12084 - (1997).
[7] Y. Chibane, B. Bouhafs, and M. Ferhat, Phys. Stat. Sol. B **240**, 116 (2003).
[8] A. Chroneos, C. Jiang, R. W. Grimes, U. Schwingenschlögl, and H. Bracht, Appl. Phys. Lett. **94**, 252104 (2009).
[9] Y. Chibane and M. Ferhat, J. Appl. Phys. **107**, 053512 (2010).
[10] N. Mousseau and M. F. Thorpe, Phys. Rev. B **46**, 15887 (1992).
[11] S. D. Gironcoli, P. Giannozzi, and S. Baroni, Phys. Rev. Lett. **66**, 2116 (1991).
[12] P. Venezuela, G. Dalpian, A. da Silva, and A. Fazzio, Phys. Rev. B **64**, 193202 (2001).
[13] A. Chroneos, H. Bracht, C. Jiang, B. Uberuaga, and R. Grimes, Phys. Rev. B **78**, 195201 (2008).
[14] E. Kasper, A. Schuh, G. Bauer, B. Holländer, and H. Kibbel, J. Cryst. Growth **157**, 68 (1995).
[15] J. Tolle, A. V. G. Chizmeshya, Y. Y. Fang, J. Kouvetakis, V. R. D'Costa, C. W. Hu, J. Menéndez, and I. S. T. Tsong, Appl. Phys. Lett. **89**, 231924 (2006).
[16] G. Kresse and J. Furthmüller, Phys. Rev. B **54**, 11169 (1996).
[17] G. Kresse and J. Hafner, J. Phys. Condens. Matter **6**, 8245 (1994).
[18] D. M. Ceperley and B. J. Alder, Phys. Rev. Lett. **45**, 566 (1980).
[19] J. P. Perdew and A. Zunger, Phys. Rev. B **23**, 5048 (1981).
[20] M. Cardona, Solid State Commun. **133**, 3 (2005).
[21] M. Bauer, J. Taraci, J. Tolle, A. V. G. Chizmeshya, S. Zollner, D. J. Smith, J. Menendez, C. Hu, and J. Kouvetakis, Appl. Phys. Lett. **81**, 2992 (2002).
[22] L. R. Doolittle, Nucl. Instr. Meth. Phys. Res. B **9**, 344 (1985).
[23] M. A. Wistey, Y. Y. Fang, J. Tolle, A. V. G. Chizmeshya, and J. Kouvetakis, Appl. Phys. Lett. **90**, 082108 (2007).
[24] H. J. McSkimin, J. Appl. Phys. **24**, 988 (1953).
[25] J. Kouvetakis, J. Menendez, and A. V. G. Chizmeshya, Annu. Rev. Mater. Res. **36**, 497 (2006).
[26] O. Madelung, *Landolt Börstein* (Springer-Verlag, Berlin, 2001), Vol. 41-Aα.
[27] D. D. Cannon, J. Liu, Y. Ishikawa, K. Wada, D. T. Danielson, S. Jongthammanurak, J. Michel, and L. C. Kimerling, Appl. Phys. Lett. **84**, 906 (2004).
[28] J. Thewlis and A. R. Davey, Nature **174**, 4439 (1954).
[29] V. R. D'Costa, Y. Fang, J. Mathews, R. Roucka, J. Tolle, J. Menendez, and J. Kouvetakis, Semicond. Sci. Technol. **24**, 115006 (2009).
[30] J. Mathews, R. T. Beeler, J. Tolle, C. Xu, R. Roucka, J. Kouvetakis, and J. Menéndez, Appl. Phys. Lett. **97**, 221912 (2010).
[31] C. Y. Fong, W. Weber, and J. C. Phillips, Phys. Rev. B **14** , 5387 (1976).
[32] Y. Cai and M. F. Thorpe, Phys. Rev. B **46**, 15872 (1992).
[33] J. C. Woicik, C. E. Bouldin, M. I. Bell, J. O. Cross, D. J. Tweet, T. M. Zhang, L. B. Sorensen, C. A. King, J. L. Hoyt, P. Pianetta, and J. F. Gibbons, Phys. Rev. B **43**, 2419 (1991).
[34] D. B. Aldrich, R. J. Nemanich, and D. E. Sayers, Phys. Rev. B **50**, 15026 (1994).
[35] J. C. Aubry, T. Tyliszczak, A. P. Hitchcock, J. M. Baribeau, and T. E. Jackman, Phys. Rev. B **59**, 12872 (1999).
[36] S. Decoster, S. Cottenier, U. Wahl, J. G. Correia, and A. Vantomme, Phys. Rev. B **81**, 155204 (2010).
[37] C. Ventura, J. Fuhr, and R. Barrio, Phys. Rev. B **79**, 155202 (2009).
[38] A. Chroneos, H. Bracht, R. W. Grimes, and B. P. Uberuaga, Appl. Phys. Lett. **92**, 172103 (2008).